SHIP MANOEUVRING PREDICTION BASED ON NUMERICAL TOWING TANK TECHNIQUE

(DOI No: 10.3940/rina.ijme.2018.a3.493)

J Yao, **X Cheng** and **Z Liu**, Key Laboratory of High Performance Ship Technology (Wuhan University of Technology), Ministry of Education School of Transportation, Wuhan University of Technology, China

SUMMARY

A practical procedure is proposed in this paper to predict ship manoeuvrability. A three degrees of freedom MMG (Japanese Manoeuvring Mathematical Modelling Group)-type model is established to simulate rudder manoeuver. Propeller thrust and rudder loads are calculated by empirical formulas, whereas the hull forces as well as moment are determined with hydrodynamic derivatives which are derived from CFD (Computational Fluid Dynamics) computations. An own developed RANS (Reynolds-Averaged Naiver-Stokes) solver on the base of OpenFOAM is applied to simulate a range of PMM (Planar Motion Mechanism) tests and Fourier analyses of the computed results are carried out to obtain the required derivatives. In order to demonstrate the effectivity of the whole procedure and the RANS computations, the US (United States) combatant DTMB 5415 is taken as a sample for an application. Forced motions of surge, sway, yaw and yaw with drift for the bare hull with bilge keels are simulated. Thereafter, simulations of standard rudder manoeuvers, i.e. turning and zigzag, are performed by applying the computed derivatives. The results are compared with available measured data. It has been shown that the present procedure together with the RANS method can be used to evaluate the manoeuvrability of a ship since general good agreements between the simulated results and measured data are achieved.

1. INTRODUCTION

The manoeuvrability is one of the important performances of a ship, closely related to navigation safety. It is usually necessary to estimate manoeuvring behaviour of a new ship form at initial design stage. Traditionally, a mathematical model with coefficients obtained from empirical database is preferred to be used to achieve the initial evaluation. The advantages are significant since it is faster, simpler and lower-cost than the approaches based on model test in a tank. However, the disadvantage is also obvious since the prediction accuracy depends heavily on the coincidence degree between the new designed ship and the ones from which the database is derived by model tests. So far there are two types of mathematical models, i.e., MMG model (Ogawa, 1977; Ogawa and Kasai, 1978) and Abkowitz model (Abkowitz, 2006). The former was developed by the Japanese research group during 1976-1980. This model takes hull, rudder and propeller into account separately, other than the latter in which the ship is considered as a whole system. The related coefficients involved in a MMG-type model can reflect specific physical meaning, e.g., hull-rudder-propeller interaction, but the Abkowitz-type model is generally expected to be more accurate. Both mathematical models are popular in applications as reported in literatures, e.g., Cura-Hochbaum (2006) and He (2016). Nowadays the use of a mathematical model remains a main approach for manoeuvring prediction, especially in the initial design phase.

The key to success in applying the empirical method to prediction of manoeuvring performance depends on how accurate the empirical coefficients are. Unfortunately, it is usually hard to get very accurate results by empirical coefficients, because different ship forms have their own unique coefficients. In recent years, as CFD techniques have become more and more mature, the concept of "numerical tank" appears. We can use this concept to simulate ship tests in a tank for manoeuver, mainly including towing tank test and free running test. The simulations using CFD techniques can generally reach a high accuracy, as concluded from the workshop SIMMAN 2008 (Stern *et al*, 2011) which is the first workshop on verification and validation of ship manoeuvring simulation methods. From the workshop, it has been also shown that direct simulation of free running model test remains extremely time consuming and several months are normally required for a case, so that in order to be more economical CFD methods are more used for the simulations of towing tests in applications up to now. As an alternative, "numerical towing tank" is undoubtedly expected to be more accurate than empirical methods. It balances well the requirement of accuracy and time cost at the initial stage of ship design.

An attempt is made herein to predict ship manoeuvrability by using a 3 degrees of freedom MMG-type model. The proposed procedure of prediction is based on a semi-CFD-based and semi-empirical approach since the propeller thrust and rudder loads in the mathematic model are calculated by empirical formulas, while the derivatives for calculation of hull force (moment) are generated by virtual PMM test. The RANS solver (Yao, 2015) developed previously on the base of OpenFOAM is used to simulate ship PMM motions, i.e., surge, sway, yaw and yaw with drift. A validation study is done for the free surface combatant DTMB 5415 model. The simulations of PMM test and the whole procedure are validated by comparing the results with available measured data. The whole procedure is demonstrated to be promising for manoeuvring prediction since the predicted results show satisfactory agreements with measured data.

2. MMG MODEL

2.1 EQUATIONS OF MOTION

Supposing a ship is seen as a rigid body and moves in horizontal plane, the ship motion consists of three basic motions, i.e., translations along x- and y-axis and rotation about z-axis where the defined coordinate system o-xyz is fixed to the ship. The origin o is located at the intersection of mid-ship sections and undisturbed free surface, x-axis towards bow, y-axis towards starboard and z-axis vertical downwards. According to Newton's law, the ship motion equations with 3 degrees of freedom can be written as

$$m(\dot{u} - vr - x_G r^2) = X \tag{1a}$$

$$m(\dot{v} + ur + x_G \dot{r}) = Y \tag{1b}$$

$$I_z \dot{r} + m x_G (\dot{v} + ur) = N \tag{1c}$$

where X, Y and N are longitudinal force, side force and yaw moment respectively, m is mass, u and v are translational velocities along x- and y-axis respectively, r is yaw rate about z-axis, x_G is x-coordinate of the centre of gravity, I_z is inertial moment with respect to z-axis and dot over quantities means the operation of derivation.

A MMG-type model is used in this study to approximate the hydrodynamic forces and moment on the right side of Eq. (1). The model has the following expressions.

$$X = X_H + X_P + X_R \tag{2a}$$

$$Y = Y_H + Y_R \tag{2b}$$

$$N = N_H + N_R \tag{2c}$$

where the subscripts H, P and R represent the force or moment acting on hull, propeller and rudder respectively. Note that the side force and yaw moment due to propeller are assumed to be zero in Eq. (2). In fact, previous study by the authors (Yao, 2015) has shown that the contribution of the propeller side force/yaw moment to the total side force/yaw moment of the whole ship system is small (generally less than one percent) and therefore it is ignored in present consideration.

2.2 PROPELLER THRUST

The propeller thrust (X_P), as well as rudder side force and yaw moment, is calculated by the similar formulas as described by Yasukawa and Yoshimura (Yasukawa and Yoshimura, 2015). For the propeller thrust, the expression is as follows.

$$X_P = (1 - t_p)\rho n^2 D^4 K_T(J_P) \tag{3}$$

where ρ is water density, t_p is thrust deduction factor when the ship travels straight ahead, D is propeller diameter, n is revolution rate, K_T is the open water characteristic and advance ratio J_P is defined as

$$J_P = \frac{u(1 - w_p)}{nD}. \tag{4}$$

Here w_p is effective propeller wake fraction which takes manoeuvring motions into account and can be estimated by

$$w_p = w_{p0} \exp(-4\beta_P^2). \tag{5}$$

In above equation, w_{p0} is the propeller wake fraction in the condition of straight ahead motion and β_P is geometrical inflow angle into propeller which is defined as

$$\beta_P = \beta - x_P' r' \tag{6}$$

where $\beta = \mathrm{atan}(-v/u)$ is drift angle, x_P' is equal to x_P/L_{pp}, x_P is x-coordinate of propeller position, L_{pp} is ship length between perpendiculars and r' is non-dimensional yaw rate, defined by rL_{pp}/u.

2.3 RUDDER LOADS

For the rudder forces (X_R and Y_R) and yaw moment (N_R) in Eq. (2), the following formulas are used to calculate them.

$$X_R = -(1 - t_R)F_N \sin\delta \tag{7a}$$

$$Y_R = (1 + \alpha_H)F_N \cos\delta \tag{7b}$$

$$N_R = Y_R x_R \tag{7c}$$

where δ is rudder angle (positive when deflected to port side), x_R is x-coordinate of the point on which Y_R acts, t_R and α_H are ratios of hydrodynamic force, induced on ship hull by rudder action, to rudder force in x and y directions respectively. The rudder normal force F_N can be written in the form

$$F_N = \frac{1}{2}\rho \frac{6.13\lambda}{\lambda + 2.25} A_R V_R^2 \sin\alpha_R \tag{8}$$

where λ is rudder aspect ratio, A_R is lateral area of rudder, V_R is effective inflow velocity of rudder and α_R is effective rudder inflow angle. V_R can be estimated by the following model as recommended by Yoshimura and Nomoto (Yoshimura and Nomoto, 1978).

$$V_R = U(1 - w_R)\sqrt{1 + G(s)} \tag{9a}$$

$$G(s) = \frac{D}{H}\frac{\kappa[2 - (2 - \kappa)s]}{(1 - s)^2} \tag{9b}$$

$$s = 1 - \frac{u(1 - w_P)}{nP} \tag{9c}$$

where H is rudder height, w_R is effective rudder wake fraction, P is propeller pitch, κ is a parameter reflecting acceleration effect of propeller and U is resultant speed of ship. w_R is computed by the below equation, similar with the one for w_P.

$$w_R = w_{R0} \exp(-4\beta_P^2) \tag{10}$$

Taking the flow-rectifying effect into account, α_R can be expressed in the form

$$\alpha_R = \delta - \delta_0 - \gamma\beta_R \frac{U}{u_R} \tag{11a}$$

$$\beta_R = \beta - 2x_R' r' \tag{11b}$$

where x_R' is x_R/L_{pp}, δ_0 is the rudder angle of zero rudder normal force, $u_R = V_R \cos\beta_R$ and γ is flow-rectification coefficient.

In the equations (3) and (7), some of involved parameters or coefficients are determined by rudder and propeller geometries, such as D, x_P, H and P, while some reflect hydrodynamic characteristics, such as γ, α_H and t_R which are usually derived from model tests or experience. In addition, the below two assumptions are introduced in above propeller and rudder models since the simplified aspects may play little roles to the whole ship system.

- The acting point of rudder side force is always located on the axis of rudder stock. This means the shift of force point caused by ship motion and/or rudder action is neglected. Thus, x_R is assumed to be constant and equal to $-0.5L_{PP}$.
- For a twin screw ship, if propeller revolution rates are same the thrusts produced by both propellers are assumed to be identical, regardless of the different disturbances of ship hull to the propeller inflow when the ship performs manoeuvring motions. For rudders, similar assumptions are adopted.

2.4 FORCE AND MOMENT ACTING ON SHIP HULL

A rather simple model is used to approximate X_H, Y_H and N_H which are expressed as

$$X_H = X_0 + X_u\Delta u + X_{uu}(\Delta u)^2 + X_{uuu}(\Delta u)^3 + X_{vv}v^2 + X_{rr}r^2 + X_{vr}vr \tag{12a}$$

$$Y_H = Y_v v + Y_{vvv}v^3 + Y_{\dot{v}}\dot{v} + Y_r r + Y_{rrr}r^3 + Y_{\dot{r}}\dot{r} + Y_{vrr}vr^2 + Y_{vvr}v^2 r \tag{12b}$$

$$N_H = N_v v + N_{vvv}v^3 + N_{\dot{v}}\dot{v} + N_r r + N_{rrr}r^3 + N_{\dot{r}}\dot{r} + N_{vrr}vr^2 + N_{vvr}v^2 r \tag{12c}$$

where $\Delta u = u - u_0$, u_0 is the ship speed which is taken as a point for Taylor series expansion.

3. APPLICATION FOR DTMB 5415

3.1 SHIP DATA

DTMB 5415 is a widely used benchmark ship for the purpose of CFD validation. A variety of measured data about manoeuver of this ship are available to check the accuracies of present computed results. The principal particulars in full and model scale are listed in Table 1. In this study, the flows around the ship at model scale are simulated to obtain hydrodynamic derivatives.

Table 1: The data of DTMB 5415

Parameters	Full scale	Model scale
Hull		
$L_{pp}\ (m)$	142	3.048
$B\ (m)$	19.06	0.409
$d\ (m)$	6.15	0.132
C_B	0.507	
$x_G\ (m)$	-0.97	-0.0208
$I_z\ (kg \cdot m^2)$	10616850100	48.375
Propeller		
No. of propeller	2	
$D\ (m)$	6.15	0.132
P/D	0.87	
x_p/L_{pp}	-0.44	
Rudder		
No. of rudder	2	
$A_R\ (m^2)$	15.4	0.007095
$H\ (m)$	6.15	0.132

3.2 DETERMINATION OF HYDRODYNAMIC DERIVATIVES

In order to obtain the hydrodynamic derivatives in Eq. (12), PMM motions including pure surge, pure sway, pure yaw and combined yaw-drift are simulated by using the RANS solver mentioned previously. The motion parameters are as follows.

Surge:

$$u = u_0 + \Delta u_{max}\cos(2\pi f t)\,,\ \Delta u_{max} = 0.1u_0 \text{ and } f = 0.1\ s^{-1} \tag{13a}$$

$$v = 0 \tag{13b}$$

$$r = 0 \tag{13c}$$

Sway:

$$u = u_0 \quad (14a)$$

$$v = v_{max}\cos(2\pi ft)\,,\ v_{max} = 0.174u_0 \text{ and } f = 0.134\ s^{-1} \quad (14b)$$

$$r = 0 \quad (14c)$$

Yaw:

$$u = u_0 \quad (15a)$$

$$v = 0 \quad (15b)$$

$$r = r_{max}\cos(2\pi ft)\,,\ r_{max} = 0.3u_0/L_{pp} \text{ and } f = 0.134\ s^{-1} \quad (15c)$$

Yaw and drift:

$$u = u_0\cos\beta\,,\ \beta = 10° \quad (16a)$$

$$v = -u_0\sin\beta \quad (16b)$$

$$r = r_{max}\cos(2\pi ft)\,,\ r_{max} = 0.3u_0/L_{pp} \text{ and } f = 0.134\ s^{-1} \quad (16c)$$

The above parameters except for the pure surge motion are accordance with the conditions of model test by IIHR-Hydroscience & Engineering-University of Iowa, where u_0 is $1.531\ m/s$ corresponding to a Froude number 0.28.

The OpenFOAM-based RANS solver used in present work has been previously applied for the simulations of double-body flows since Froude numbers were low, less than 0.2. The previous work has shown that the methodology of RANS is effective to simulate ship PMM motions and of enough accuracy. In present case, the Froude number is relatively large, so that the method is further used for free surface flow by using the VoF method (Volume of Fluid). In all computations, the ship is fixed to heave, pitch and roll. The related methods including governing equations of fluid dynamics, boundary conditions, and so on, have been already described in previous publication (Yao, 2015), so the same will not be repeated here.

Present computational domain is limited in a box in size of $-2.5 \le x/L_{pp} \le 1.5$, $-2.0 \le y/L_{pp} \le 2.0$ and $-0.5 \le z/L_{pp} \le 1.0$. The software NUMECA Hexpress is used to generate an unstructured grid around the model for the computations. Figure.1 presents a half of the grid. In order to more accurately capture the free surface, the mesh near the free surface is refined in the three directions of space.

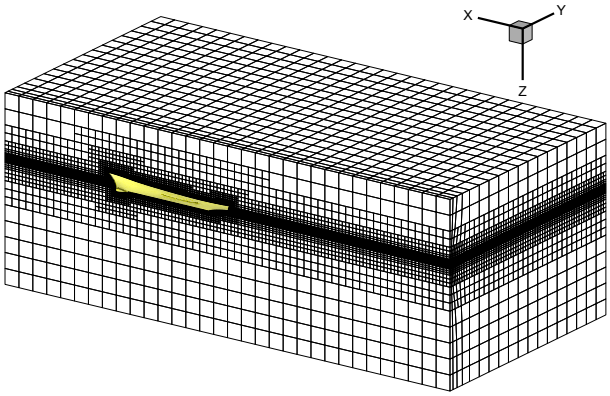

Figure.1 Half computational grid on the starboard side of DTMB 5415 model

A grid dependency study is firstly carried out for the static drfit case $\beta = 20°$. The reasons are that the selected case is expected to be able to reflect a general conclusion of grid dependency study and the run time for a static case is much shorter than that required for a dynamic case. A coarse, a medium and a fine are generated by systematically increasing grid density in three directions. The resulting grids have around 0.52, 1.22 and 2.6 million cells respectively. Since wall function is used to model near-wall turbulence during computations, the thickness of the first grid point to hull should satisfy the condition that y^+ locates in log-layer, usually $y^+ > 30$. According to a few pre-computations, the range of y^+ is between around 40 and 150 for all grids after adjusting the thickness of the wall-adjacent cells.

Table 2 Results from grid dependency study

	coarse	medium	fine
X'_H	-0.0267 -4.98%	-0.0281 -2.75%	-0.0289 ---
Y'_H	0.156 2.63%	0.152 1.33%	0.150 ---
N'_H	0.0526 1.54%	0.0518 -0.58%	0.0521 ---

For these computations, the time step is set to be 0.01s and it needs to run up to around 50s for a good convergent result. Table 2 lists the computed longitudinal force, side force and yaw moment including the convergence analysis. X_H, Y_H and N_H are made to be non-dimensional by

$$Force' = \frac{Force}{0.5\rho u_0^2 L_{pp} d} \quad (17a)$$

$$Moment' = \frac{Moment}{0.5\rho u_0^2 L_{pp}^2 d}. \quad (17b)$$

It is seen that the grids show a good convergence since with refinement of grid the changes of X_H, Y_H and N_H become smaller. However, there remains a discrepancy of around 3% between the longitudinal forces based on the medium and fine grids. The side force and moment are not so sensitive to grid refinement as the longitudinal force shows.

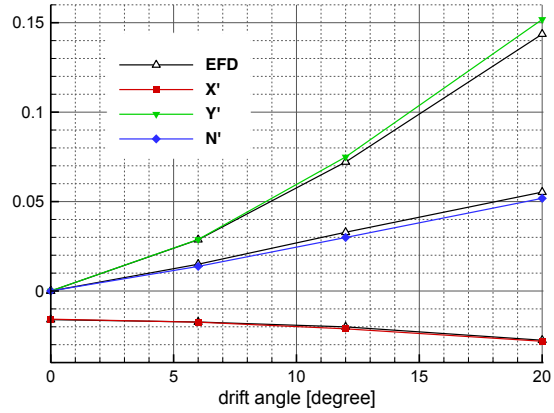

Figure.2 Comparison of computed results with measured data for static drift

In view of above comparisons, using the medium grid may obtain results with enough accuracy. To demonstrate that, the medium grid is firstly used for other drift cases at $\beta = 0°,\ 6°,\ 12°$. When $\beta = 0°$, i.e., resistance, because of symmetric flow only half computational domain is considered to reduce computational time. For a case of non-zero drift angle, the computation requires around 1.5 day to reach the convergent solution when using 16 processors on a small workstation. Figure. 2 shows a comparison of the computed results with the experimental data published by IIHR on SIMMAN 2008. At a small drift angle, e.g. $\beta = 6°$, the side force and yaw moment agree excellently with the EFD (Experimental Fluid Dynamics) data, however, the absolute error becomes generally larger as drift angle increases. The computations overestimate the side forces at all drift angles, but underestimate all yaw moments. At $\beta = 20°$, the error is around 5.69% for side force and around -6.31% for yaw moment. The largest error for longitudinal force is around 5.4% at $\beta = 12°$.

Moreover, the plots in Figure.2 are fitted by polynomials (second-order for longitudinal force and three-order for others) to derive the v-related derivatives. The resulting non-dimensional derivatives are presented in Table 3. We can see that the linear derivatives agree well with experimental data from SIMMAN, however, for high-order derivatives errors are relatively large.

Table 3 Derivatives from static drift

	X'_0	X'_{vv}	Y'_v	Y'_{vvv}	N'_v	N'_{vvv}
EFD	-0.0161	-0.194	-0.296	-6.561	-0.153	-0.498
CFD	-0.0157	-0.160	-0.302	-7.530	-0.138	-0.752

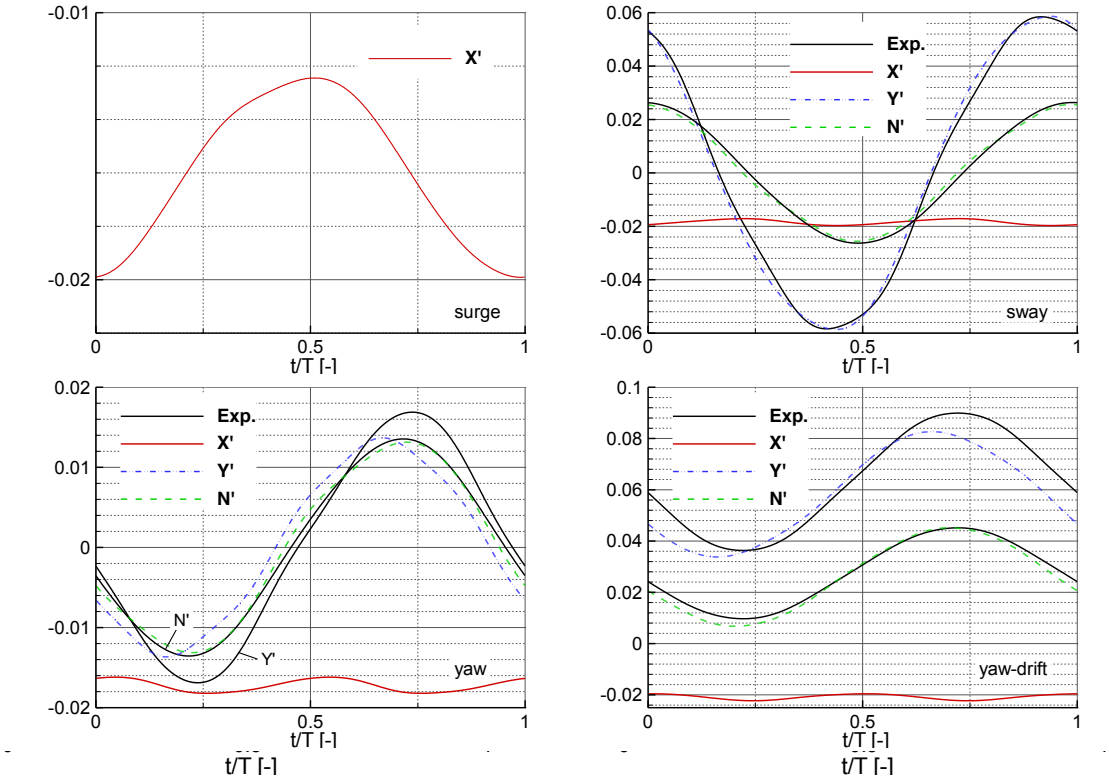

Figure.3 Time histories of force and moment over one period during PMM motions

We have, as yet, a strong confidence to simulate the PMM motions by using the RANS solver. Here the medium grid is still used and time step remains 0.01s. Around 2.5 days are consumed in the computation of one period sway motion, as well as of one period yaw and yaw-drift motions, using 16 processors. For surge, again only half computation domain is considered for the purpose of time reduction due to symmetric flow.

The computed time histories of non-dimensional longitudinal force, side force and yaw are presented in Figure.3. The available measured data is plotted in the figure as well. Unfortunately, there is not measured data for surge. For the sway, the side force and yaw moment show excellent agreements with the measured data. But for the yaw and yaw-drift, good agreements are only for the yaw moments and the side forces display a phase lead relative to the measured curves. It should be pointed that the measured longitudinal forces, which are not shown in the figure, are most probably wrong as concluded from SIMMAN and differs remarkably from the computed ones. The reason may be due to the difficulties to accurately measure the force during dynamic motions. So that for this situation static cases, such as drift and turning, are usually recommended when testing in a tank.

Analysing the results in Figure. 3 by means of Fourier series and comparing coefficients on the right-hand and left-hand sides of Eq. (12), we can obtain the required derivatives, which are listed in Table 4. The deviation of CFD-based derivatives to experiment is obvious, especially for high-order and coupled derivatives, which is due to the error of CFD results, as compared in Figure. 3. Note that the measured derivatives in red bold font, i.e., *X*-related ones, are from the source data on SIMMAN depending on model tests of static PMM motions.

On the other hand, the corresponding linear derivatives in Tables 3 and 4 present a small difference, rather than the high-order derivatives showing a larger discrepancy. Note that the derivatives in Table 3 are derived from static drift test, whereas those in Table 4 are from dynamic tests, e.g. sway. There is normally small difference between them. Generally speaking, the derivatives based on static tests are considered to be more accurate. However, we use the derivatives from dynamic tests for the comparison purpose in this study. The empirical coefficients involved in the MMG-type model, are also given in the back of Table 4. These coefficients are determined by ship form, such as, block coefficient and *Lpp*/*B*. The coefficients for K_T are from experiment, released on SIMMAN.

3.3 SIMULATION OF RUDDER MANOEUVER

With the resulting derivatives and model coefficients in Table 4, the zigzag manoeuver $-20°/20°$ is firstly simulated. According to the measured data, the simulation of free running test is performed by solving Eq. (1), then all data is transformed to full scale using ship velocity and length. The time is discretized by a second-order Runge-Kutta scheme. First-order Euler scheme may be used as well since ships usually perform weak inertial motions. The ship speed is 18 kn and rudder rate is $9°/s$. The results are shown in Figure. 4. As indicated, both results based on PMM test are close to that based on free running test. The CFD-PMM-based rudder angle and heading angle have a time lead relative to that based on free running test. This is also observed for the EFD-PMM-based rudder angle and heading angle, but more severe. The same feature is also found for the turning rate in the right view in Figure. 4. More details of the analysis parameters are shown in Table 5. We can conclude that the results derived from both real and virtual PMM tests are acceptable because the prediction errors are generally small. However, it is hard to say which prediction is better since not all parameters are superior.

Table 4 Derivatives and empirical coefficients

	CFD	EFD
surge		
X'_0	-0.0158	**-0.0161**
X'_u	-0.0371	**-0.0088**
X'_{uu}	-0.042	**-0.022**
X'_{uuu}	0	**0**
$X'_{\dot{u}}$	-0.0044	**0**
sway		
X'_{vv}	-0.0746	**-0.194**
Y'_v	-0.258	-0.273
Y'_{vvv}	-1.587	-2.979
$Y'_{\dot{v}}$	-0.106	-0.0955
N'_v	-0.131	-0.148
N'_{vvv}	-0.524	-0.121
$N'_{\dot{v}}$	-0.0115	-0.00807
yaw		
X'_{rr}	-0.0222	**-0.0132**
Y'_r	-0.0268	-0.0448
Y'_{rrr}	-0.176	-0.132
$Y'_{\dot{r}}$	-0.0127	-0.0158
N'_r	-0.0359	-0.0398
N'_{rrr}	-0.0829	-0.0474
$N'_{\dot{r}}$	-0.00803	-0.00709
yaw-drift		
X'_{vr}	-0.0311	**0.0819**
Y'_{vvr}	-1.01	-1.517
Y'_{vrr}	-0.912	-0.868

N'_{vvr}	-0.639	-0.722
N'_{vrr}	-0.164	-0.199
Empirical coefficients		
α_H	0.2	
t_R	0.15	
t_p	0.1	
w_{p0}	0.1	
w_{R0}	0.12	
κ	0.4	
γ	0.8	
K_T	$0.398 - 0.0678J_p - 1.286J_p^2 + 2.287J_p^3 - 2.04J_p^4 + 0.676J_p^5$	

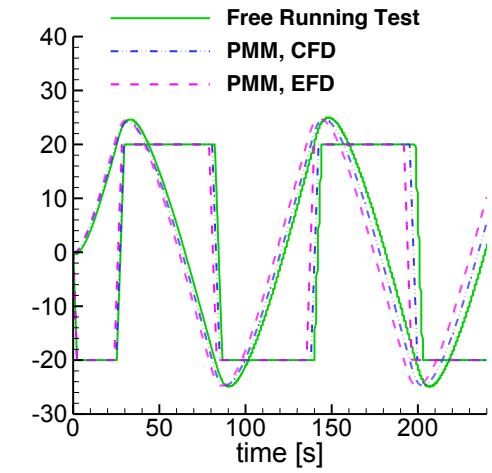

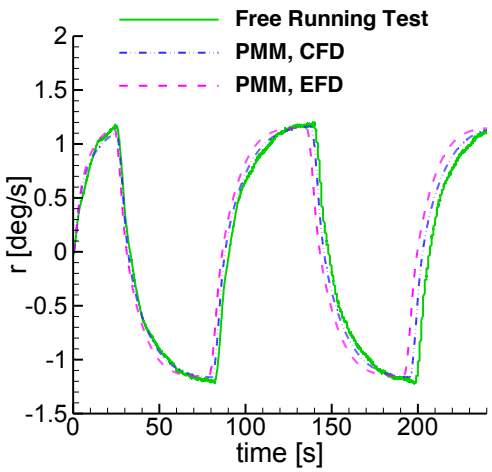

Figure.4 Comparison of results for zigzag manoeuver $-20°/20°$

Table 5 Characteristic parameters from zigzag manoeuver $-20°/20°$

Parameters	Free running test	PMM, EFD	PMM, CFD
Rudder execute time (s)			
2nd	25.4	23.9	25.0
3rd	82.3	78.9	80.7
4th	140.0	135.5	138.0
5th	198.8	192.0	195.3
Overshoot angle (deg)			
1st	4.5	4.53	4.26
2nd	4.9	4.76	4.72
3rd	4.9	4.76	4.72
4th	4.9	4.76	4.72
Overshoot time (s)			
1st	8.7	7.1	6.8
2nd	8.3	7.7	7.5
3rd	7.6	7.6	7.5
4th	7.3	7.8	7.5
Max turning rate (deg/s)			
1st	1.16	1.14	1.1
2nd	-1.2	-1.15	-1.16
3rd	1.18	1.15	1.16
4th	-1.21	-1.15	-1.16

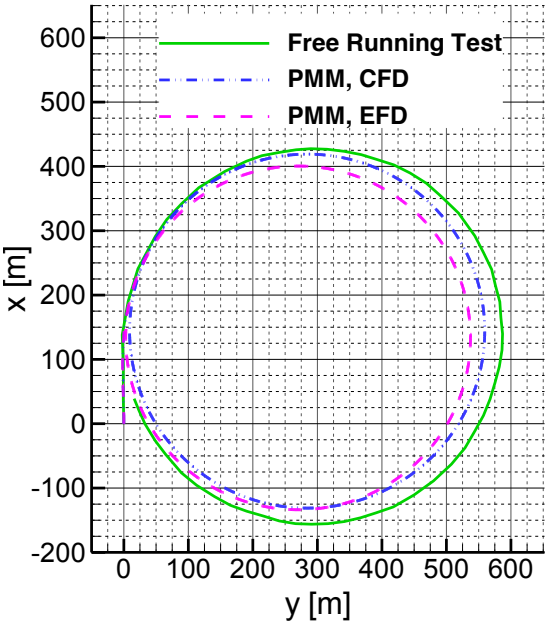

Figure.5 Comparison of turning circles $\delta = -35°$

Thereafter, Eq. (1) is solved for the prediction of turning circle manoeuver. Figure. 5 shows a comparison of the trajectories obtained from $-35°$ rudder manoeuver. The

circle based on CFD-PMM test is even closer to the measured one than the one based on CFD-PMM test. However, except for the characteristic parameters of turning circle as shown in Table 6, for other parameters of interest, such as the time of heading change (T90, T180 and T360), the predictions based on EFD-PMM test show better accuracies on the whole.

Table 6 Characteristic parameters from turning circle manoeuver $\delta = -35°$

Parameters	Free running test	PMM, EFD	PMM, CFD
Advance (m)	421.6	393.0	411.27
Transfer (m)	239.3	208.29	219.93
Tactical diameter (m)	581.3	529.89	551.70
Turning diameter (m)	587.1	534.35	550.31
T90 (s)	68.1	63.1	60.9
T180 (s)	132.0	123.8	115.7
T360 (s)	258.3	245.5	225.6
Stable turning rate (deg/s)	1.42	1.48	1.55
Stable velocity (m/s)	7.3	6.89	7.86
Stable drift angle (deg)	12.4	13.55	13.55

Note that as shown in Table 4 many derivatives have a very large error compared with measured data, but the predictions of manoeuver based on both series derivatives are surprising similar, even very close. This should be not a surprise since linear derivatives always play main roles to manoeuvrability and it is lucky that most CFD-based linear derivatives are relatively closer to the measured ones.

4. CONCLUSIONS

A procedure based on virtual PMM test to predict ship manoeuvrability is proposed. The description of method is presented in the paper. The DTMB 5415 ship is taken as an example to validate the present involved approaches. It concludes that the CFD-based derivatives can be used for manoeuvring prediction and some results are even better than that based on EFD-based derivatives. Regarding the PMM test (real and virtual), the motions of heave, pitch and roll are ignored, however, those are usually expected to have impacts on the predicted quality. On the other hand, it seems considering only a 3 degrees of freedom mathematic model is enough accurate for the sample ship although ship speed is not so low as Froude number is 0.28.

In order to check manoeuvrability of a new ship at initial design stage, the present procedure and CFD method have displayed a promising application. It can help to clear the main manoeuvring performance of a ship. Improvements in prediction can be achieved by using a more sophisticated model and taking ship posture in RANS computations into account, but also requiring more run time.

5. ACKNOWLEDGEMENTS

This work was supported by National Natural Science Foundation of China (Grant No. 51609188, 51609187, 51609186, 51479150, 51709213, 51720105011).

6. REFERENCES

1. OGAWA A., KOYAMA, T. and KIJIMA, K. *MMG report-1, on the mathematical model of ship manoeuvring*[R]. Japan: the bulletin of society of naval architects of Japan, 1977, 575:22-28.
2. OGAWA, A. and KASAI, H. *on the mathematical model of manoeuvring motion of ship*[J], International shipbuilding progress, 1978, 25(292): 306-319.
3. ABKOWITZ, M. A. *Lectures on ship hydrodynamics: steering and manoeuvrability*[R], HyA Report, 2006, No. Hy-5, Lyngby, Denmark.
4. CURA-HOCHBAUM, A. *virtual PMM tests for manoeuvring prediction*[C], 26th symposium on naval hydrodynamics, 2006, Rome.
5. HE, S., KELLETT, P. et al. *Manoeuvring prediction based on CFD generated derivatives*[J], Journal of hydrodynamics, 2016, 28(2): 284-292.
6. STERN, F., AGDRUP, K. et al. *Experience from SIMMAN 2008-the first workshop on verification and validation of ship manoeuvring simulation methods*[J], Journal of ship research, 2011, 55(2): 135-147
7. YAO, J. X., 2015. *On the propeller effect when predicting hydrodynamic forces for manoeuvring using RANS simulations of captive model tests*, Doctoral Dissertation of Technical University of Berlin, Germany
8. YASUKAWA, H. and YOSHIMURA, Y., *Introduction of MMG standard method for ship manoeuvring prediction*[J], Journal of marine science and technology, 2015, 20: 37-52.
9. YOSHIMURA,Y. and NOMOTO, K. *Modelling of manoeuvring behaviour of ships with a propeller idling, boosting and reversing*[J], Journal of the society of naval architects of japan, 1978, 144: 57-69.

